University of Nevada, Reno

Mitigation of Electromagnetic Interference in Pulse Width Modulated Voltage Source Inverters and Communication Enhancement in Power Lines

A thesis submitted in partial fulfillment of the
requirements for the degree of Master of Science in
Electrical Engineering

By

Ramesh Mulupuri
Dr. Andrzej M. Trzynadlowski /Thesis Advisor

December, 2010

University of Nevada, Reno
Statewide • Worldwide

THE GRADUATE SCHOOL

We recommend that the thesis
prepared under our supervision by

RAMESH MULUPURI

entitled

Mitigation Of Electromagnetic Interference In Pulse Width Modulated Voltage Source Inverters And Communication Enhancement In Power Lines

be accepted in partial fulfillment of the
requirements for the degree of

MASTER OF SCIENCE

Dr. Andrzej M. Trzynadlowski, Advisor

Dr. Cristian Lascu, Committee Member

Dr. Sergiu Dascalu, Graduate School Representative

Marsha H. Read, Ph. D., Associate Dean, Graduate School

December, 2010

ABSTRACT

Most of the modern society's conveniences depend on electrical energy. The power supplied by the system can be considered as raw power and often it must be conditioned according to the application. The conditioning process is done by power electronic converters using semiconductor switches. This work involves the operation of pulse width modulated inverters. Because of the high switching rate of the semiconductor switches harmonics are generated in the output voltage and current of the inverter. These harmonics result in propagation of electromagnetic noise in the power electronic system. This work explains how the harmonic pollution can be mitigated by randomizing the switching period of the pulse width modulated inverter. In particular, an advanced spectral shaping technique is presented, which produces spectral nulls at selected frequencies. The spectral nulls can then be used as communication channels in power line communication systems.

ACKNOWLEDGEMENT

First of all, I would like to thank my advisor, Dr. Andrzej M. Trzynadlowski, for his patience, continuous help, and support during my research work of this thesis. Dr. Trzynadlowski helped me to understand the basic and advanced techniques of pulse width modulation, and has guided me in the right direction by giving me great advices in my study. I am very grateful to have a chance working with such a knowledgeable professor.

I would also like to thank Dr. Cristian Lascu, whose research has been related to this thesis, for his valuable suggestions, and also for sharing his knowledge and experience with me.

I also want to express my gratitude to Dr. Sergiu Dascalu who, in spite of his very busy schedule, kindly accepted my request to be a member of my graduate committee.

Table of Contents

LIST OF FIGURES

NOMENCLATURE

L	Inductance
C	Capacitance
f	frequency
a	switching variable
b	switching variable
c	switching variable
v_{AB}	Voltage between lines A and B
v_{BC}	Voltage between lines B and C
v_{CA}	Voltage between lines C and A
V_i	DC supply voltage
v_{AN}	Voltage between line A and neutral
v_{BN}	Voltage between line B and neutral
v_{CN}	Voltage between line C and neutral
K_v	Voltage gain

$v_{LL,1,p(max)}$	maximum peak value of the output fundamental line-to-line voltage
M	magnitude control ratio, modulation index
X_C	Capacitive reactance
X_L	Inductive reactance
$d(t)$	Duty ratio
$F(t)$	Modulation function
N	ratio of switching frequency to the fundamental frequency
τ_{sw}	switching interval
f_{sw}	Switching frequency
t_m	m^{th} interval
γ_k	time between m^{th} interval and k^{th} interval
δ_k	the time from m^{th} interval to k^{th} interval
$R(\tau)$	auto correlation function
$S(f)$	spectral density function
$S_{ab}(f)$	power spectral density of the per unit line to line voltage
$S_a(f)$	power spectral density of the per unit line to neutral voltage

$E(x)$	statistical average (expectation)
Δ	random pulse position respect to the beginning of period
δ	Dirac impulse
D_x, D_y, D_z	duty cycles of the respective integer voltages
k	randomly selected from a pool of 10 distinct integer values
k_{av}	average of the k values.
$f_{sw,\,avg}$	average switching frequency
D	duty cycle
f_s	sampling frequency
f_0	cancellation frequency

Chapter 1

Introduction

Most of the modern society's conveniences depend on electrical energy. Power electronics can be viewed as a branch of electrical engineering, used to control and convert electric power using semiconductor switches. The powers systems supply a fixed ac voltage. Domestic applications use single phase, low voltage power whereas industries use three phase power with various voltage levels. The power supplied by the power system can be considered as raw power and it must be conditioned according to the application. The process of conditioning involves power conversion from ac to dc or dc to ac, and controlling of magnitude and frequency of the voltages and currents. So power electronics plays a very important role in domestic and industrial power environments.

In the past, power electronic systems were using mercury-arc rectifiers. Then rotating electro-machine converters were used for controlling and conversion of electric power. The present day's power electronics began with the silicon-controlled rectifier (SCR), developed by the General Electric Company. The SCR is a semi-controlled switch, inconvenient for dc-input power electronic converters, which is explained in Chapter 2. Present power electronic converters use fully controlled switches, such as gate turn-off thyristors (GTOs), bipolar junction transistors (BJTs), power metal oxide semiconductor field effect transistors (power MOSFETs), and insulated-gate bipolar transistors (IGBTs). The four types of power electronic conversion are ac-to-dc, dc-to-dc,

ac-to-ac and dc-to-ac. Converters employed to convert power from ac to dc are called rectifiers, the dc-to-dc conversion is realized in choppers, voltage controllers and cycloconverters perform the ac-to-ac conversion, and converters for dc-ac power conversion are called inverters.

The presented work concerns inverters, which are described in Chapter 2. The simple square-wave operation of the inverter results in distorted output current waveforms. Pulse width modulation techniques are therefore used in order to improve the quality of the current of the inverter. However, the high-frequency switching results in high harmonics of the output voltage and current, which cause electromagnetic interference (EMI). Generally, mitigation of EMI is a serious challenge and power electronic converters are one of the strongest sources of EMI. Trains of electric power pulses result in harmonics of voltage and current concentrated around the multiples of switching frequency. The fast state transitions of the power switches (during turn-on and turn-off) also result in high frequency electromagnetic noise. Because of the rapid voltage changes transient charge currents are generated in inter-wire capacitances of the cables, p-n junctions of power diodes and intra-winding capacitances of the transformers, and also transient circuit to ground currents through parasitic capacitances. Power electronic systems and communication system are often associated because power control needs information exchange. Communication signals are often sent directly in power lines. This arrangement is termed power-line communications (PLC).

Power electronic systems can be seen in many important applications like uninterruptable power supplies, renewable energy sources, electric motor drives and

many more. It is estimated that by the end of the decade more than half of the whole electric power in U.S. will flow through power electronic converters. Thus the electromagnetic interference produced by the converters becomes a serious problem. Special filters are necessary for mitigating EMI as it is unfavorable for communication systems.

EMI filters are simple circuits consisting of inductors and capacitors. These filters have insertion loss, which is approximately proportional to LCf^2, where L is the total inductance, C is the total capacitance and f is the frequency. Insertion loss depends on frequency, which implies that EMI filters are not very effective in reducing the effect of harmonics in PWM converter circuits. The switching frequencies in present PWM converters are less than 20 kHz and the voltage and current harmonic, which tend to decrease with frequency, are a major problem in the lower portion of radio frequency range. In order to eliminate these harmonics high LC valued filters are required, which makes them bulky and expensive.

In order to mitigate the harmonic pollution caused by the PWM converters, random pulse-width modulation (RPWM) techniques were proposed in [1]. PWM converters operate with width-modulated pulses of voltage. The voltage pulses appear in sequential time intervals, called switching intervals, and duration of a switching interval is called a switching period. The switching period is constant in most of the existing commercial inverters, that is, the switching frequency (a reciprocal of the switching period) is maintained constant. Switching frequency is also called a switching rate. In the RPWM techniques, the switching period is randomized in order to transfer discrete

harmonic power [watts] to continuous spectral density [watts/hertz]. Studies have shown that RPWM technique reduces EMI level by approximately 10 -20 dB [2], [3].

Novel techniques for randomizing the switching periods are discussed in Chapter 3. The randomizing is done in such a way that spectral nulls are produced at a specified frequency f_0 and its multiples. The spectral nulls have a high signal to noise ratio, allowing the nulls to be used as communication channels. The necessary conditions and the limitations of the spectral-null PWM (SNPWM) method are discussed in Chapter 3, and the details of realization of that method are described in Chapter 4. Designing random switching patterns for an inverter allows the spectrum of electromagnetic noise to be actively shaped without using any extra hardware.

Computer simulations of the SNPWM technique are described in Chapter 5. The simulation software for the project should be flexible, easy to develop and implement, and capable of supporting power system models, signal processing and spectral analysis. It should also allow for graphic representation of processed data. The popular Matlab software package was selected. Matlab provides tools for spectral analysis, simulation of power electronic converters, and graphics. For spectral analysis, the power spectral density (PSD) estimation is needed. Matlab offers a number of nonparametric and parametric methods, and eigen analysis algorithms. After some testing, the nonparametric Welch method with the Kaiser or Blackman windowing, and the multitaper method (MTM)' for PSD estimation were decided on. Results obtained using these methods are summarized in the concluding Chapter 6.

Chapter 2

Inverters and Their Control

In this chapter, basic concepts of inverters are presented. Control techniques used in inverters are explained. Problems caused by these techniques are briefly described.

2.1 Inverters

Inverters are power electronic converters used for converting dc power to ac power. The inverters are supplied by dc voltage and the output is ac voltage, whose amplitude and frequency are adjustable. Based on the type of source the inverters can be described as voltage-source inverters (VSIs) and current-source inverters (CSIs). VSIs are most commonly used. Usually, uncontrolled (diode) rectifiers are used to supply the dc power to the inverters with an LC filter (also called a dc link) as shown in Figure 2.1. The inductor blocks the high frequency component of the rectifier output current, and capacitor acts as a voltage source because the voltage across it cannot change instantaneously.

Practically inverters are built with single phase and three phase outputs, even though they can be built to produce any number of output phases. Initially SCRs (semi controlled switches) were used in power inverters. But SCRs required commutating circuits in order to turn off. These commutating circuits increased the size and cost of the inverters. Therefore, fully controlled semiconductor power switches, such as IGBTs

(insulated-gate bipolar transistors) and GTOs (gate turn-off thyristors), are now mostly used in inverters.

The inverter in Figure 2.1 is based on IGBTs. The power is taken from the ac three phase lines and fed to the rectifier in order to convert to dc power. The LC filter helps to suppress the high frequency currents and the capacitor acts as voltage source for the inverter. The three phase inverter converts the dc power to ac power.

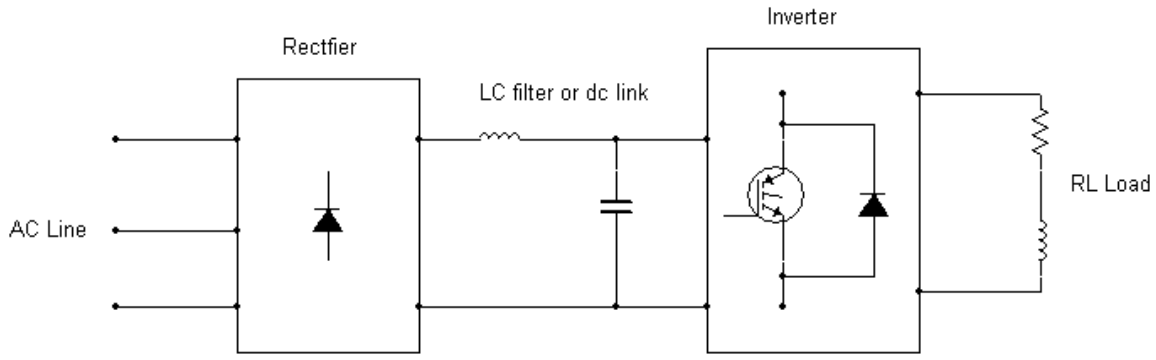

Figure 2.1: Voltage-source inverter supplied from an uncontrolled rectfier.

2.2 Inverter Operation

Figure 2.2 shows the voltage-source inverter circuit that was used in simulations and experiments. The IGBTs are used as switches and denoted by SA, SA1, SB, SB1, SC and SC1. The resistance and inductor represent an RL load.

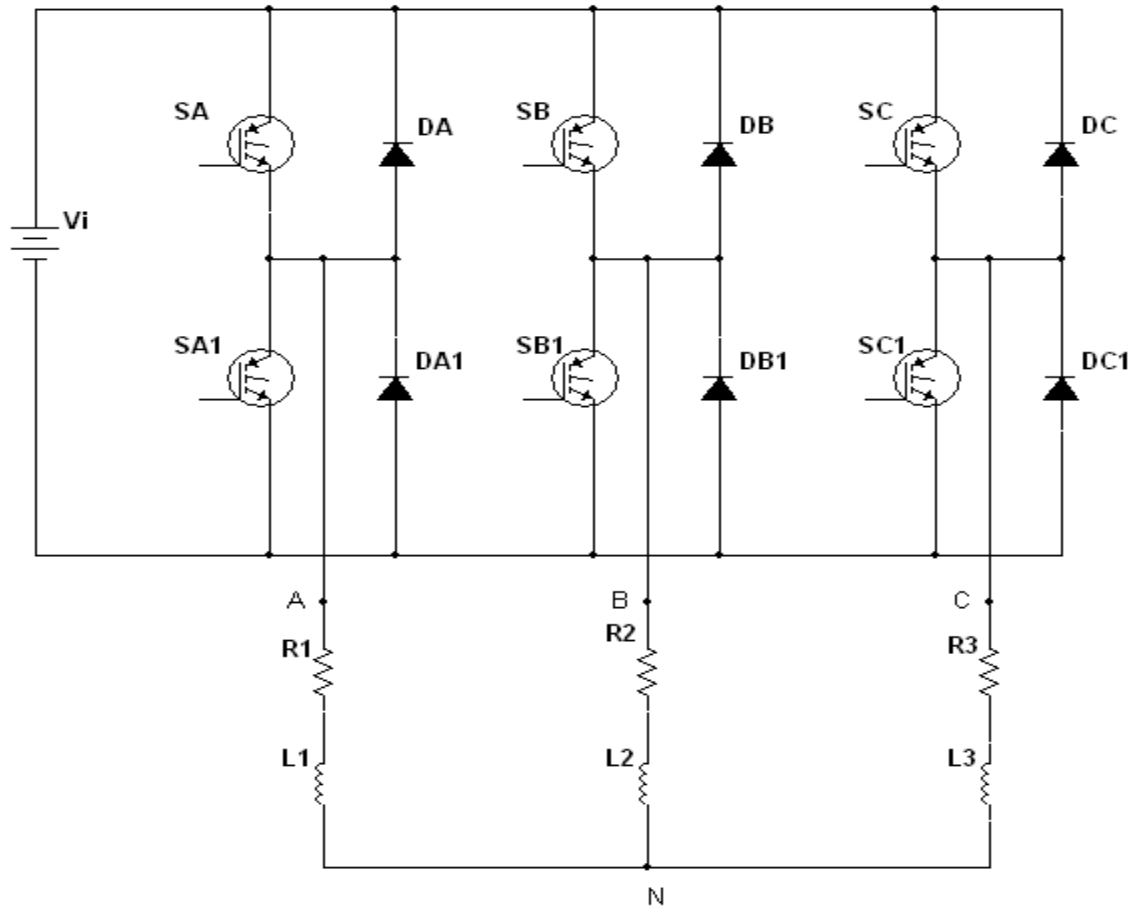

Figure 1.2: Voltage-source inverter circuit.

The three legs containing switches are represented by three switching variables: *a* (for SA and SA1), *b* (for SB and SB1) and c (for SC and SC1). Two switches from the same leg cannot be in ON at the same time. If two switches are ON in the same leg, it would short the power supply. This condition is known as shot-through. In order to avoid shot-throughs, switches are turned off shortly before turning on of the other switch in the same leg. The time interval between turn off and turn on the switches in the same leg is called blanking or dead time. Since the load contains inductance (energy storing component) diodes (DA, DA1, DB, DB1, DC and DC1) are used, in order to create a path

for the power stored in the inductor to be delivered to the power supply when the two switches in the same leg are off. These diodes are called freewheeling diodes.

Depending on the values of the switching variable *a*, *b* and *c* we can determine which switch is on. If *a* = 1, SA is ON and SA1 is OFF and if *a* = 0, SA is OFF and SA1 is ON. If *b* = 1, SB is ON and SB1 is OFF and if *b* = 0, SB is OFF and SB1 is ON. If *c* = 1, SC is ON and SC1 is OFF and if *c* = 0, SC is OFF and SC1 is ON. The line-to-line voltages are v_{AB} (voltage between A and B in Figure 2.2), v_{BC} (voltage between B and C), and v_{CA} (voltage between C and A). The values of these voltages are given by

$$\begin{bmatrix} v_{AB} \\ v_{BC} \\ v_{CA} \end{bmatrix} = V_i \begin{bmatrix} 1 & -1 & 0 \\ 0 & 1 & -1 \\ -1 & 0 & 1 \end{bmatrix} \begin{bmatrix} a \\ b \\ c \end{bmatrix} \tag{2.1}$$

where V_i denotes the dc supply voltage.

Therefore, the line-to-line voltages can only assume values of V_i, 0, or -V_i. The line-to-neutral voltages are v_{AN} (voltage between A and N in Figure 2.2), v_{BN} (voltage between B and N), and v_{CN} (voltage between C and N). The line-to-neutral voltages are given by

$$\begin{bmatrix} v_{AN} \\ v_{BN} \\ v_{CN} \end{bmatrix} = \frac{V_i}{3} \begin{bmatrix} 2 & -1 & -1 \\ -1 & 2 & -1 \\ -1 & -1 & 2 \end{bmatrix} \begin{bmatrix} a \\ b \\ c \end{bmatrix} \tag{2.2}$$

Depending upon the values of the switching variable *a*, *b* and *c*, eight different states are possible. There are two zero states: state 0 when all the variables are 0 and state

7 when all the variables are 1. From Eqs. (2.1) and (2.2) it can be seen that all the line-to-line and line-to-neutral voltages are then 0. The other six states (state 1 to state 6) produce non-zero voltages. Generally, a state can be denoted by a decimal number abc2. Thus, state 1 = 001, state 2 = 010, state 3 = 011, state 4 = 100, state 5 = 101, and state 6 = 110.

In order to obtain balanced 3-phase output from the inverter, it must repeatedly follow the sequence of states 5-4-6-2-3-1. The frequency of repetition dictates the fundamental frequency of output voltages. This mode of operation of inverter is called a square wave mode. The output current of the square wave mode of operation of the inverter is distorted. In order to improve the output current quality pulse width modulation (PWM) technique is used. In the PWM mode, the inverter switches are turned ON and OFF many times per switching cycle, and the duty ratio of switching pulses varies throughout the switching cycle. The value of the so-called modulation index affects the magnitude of the output voltages. The switching frequency is set to a value (usually several kHz), which constitutes a compromise between the high quality of output current and possibly low switching losses in the inverter switches.

2.3 Pulse Width Modulation Techniques

The amplitude and frequency of the fundamental output voltage constitute control variables in voltage controlled inverters. The most commonly used PWM techniques are the voltage space-vector PWM, carrier-comparison PWM, and modulating-function PWM. A PWM technique for a three phase inverter is expected to have the following characteristics

1. The dc supply voltage should be utilized effectively with a high value of voltage gain K_V, which is given by

$$K_v = \frac{v_{LL,1,p(max)}}{v_{\mathrm{i}}} \tag{2.3}$$

where $v_{LL,1,p(max)}$ is the maximum peak value of the output fundamental line-to-line voltage.

2. Voltage control must be linear, that is,

$$v_{LL,1,p}(M) = M\, v_{ll,1,p(max)} \tag{2.4}$$

where M is the magnitude control ratio.

3. The amplitude of the lower order harmonics should be possibly low in order to reduce the harmonic content of the output current.
4. Switching losses of the inverter switches should be possibly low.
5. For the proper operation of inverter switches, a sufficient switching time must be ensured.

2.4 Voltage Space-Vector PWM Technique

In the described study, the popular voltage space-vector PWM technique has been employed. The voltage space vectors concept is derived from the theory of electric ac machines. Three-phase voltages are converted to two-dimensional space vectors in the complex (D, jQ) plane. The voltage space vector $\boldsymbol{V}$ is defined as

$$\boldsymbol{V} = v_{\mathrm{D}} + jv_{\mathrm{Q}} \tag{2.5}$$

The conversion of the three to two dimensions lead to no loss of information because only two out of three voltages are independent. For example, considering the line-to-neutral voltages v_{AN} and v_{BN} as independent, the third voltage, v_{CN} is given as, $v_{CN} = - v_{AN} - v_{BN}$. The ABC-to-DQ transformation is

$$\begin{bmatrix} v_D \\ v_Q \end{bmatrix} = \begin{bmatrix} 1 & -\frac{1}{2} & -\frac{1}{2} \\ 0 & \frac{\sqrt{3}}{2} & -\frac{\sqrt{3}}{2} \end{bmatrix} \begin{bmatrix} v_{AN} \\ v_{BN} \\ v_{CN} \end{bmatrix} \tag{2.6}$$

Generally the ac voltages are expressed as sinusoids, for the explanation of voltage space-vector PWM techniques ac voltages are expressed as cosinusoids. The fundamental line-to-neutral output voltage of the three phases can be represented as

$$v_{AN,1}(\omega t) = v_{LN,1,p} cos(\omega t) \tag{2.7}$$

$$v_{BN,1}(\omega t) = v_{LN,1,p} cos(\omega t - \frac{2\pi}{3}) \tag{2.8}$$

$$v_{CN,1}(\omega t) = v_{LN,1,p} cos(\omega t + \frac{2\pi}{3}) \tag{2.9}$$

The peak value of these voltages is $V_{LN,1,p}$. Using Eq. 2.6, the voltage vector $\boldsymbol{v}_{LN,1}$ can be expressed as

$$\boldsymbol{v}_{LN,1} = \frac{3}{2} v_{LN,1,p} cos(\omega t) + j\frac{3}{2} v_{LN,1,p} sin(\omega t) \tag{2.10}$$

$$\boldsymbol{v}_{LN,1} = \frac{3}{2} v_{LN,1,p} e^{j\omega t} \tag{2.11}$$

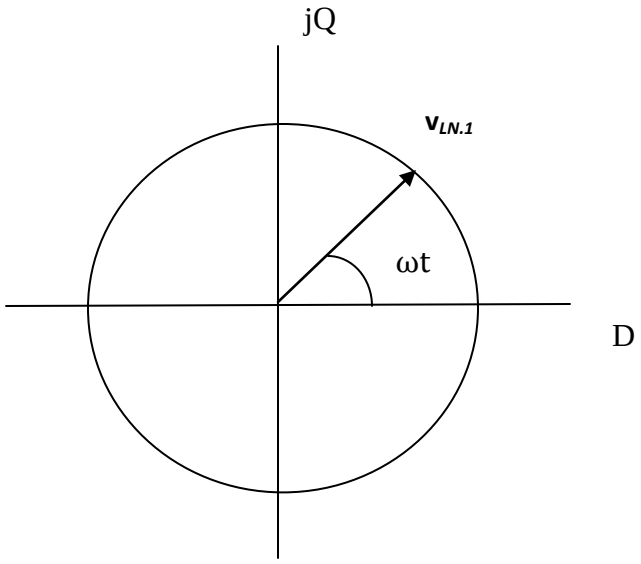

Figure 2.3: Fundamental line-to-neutral voltage vector.

Eqs. 2.10 and 2.11 represent the phasor and polar form of $\boldsymbol{v_{LN,1}}$ respectively. Thus the line-to-neutral voltage vector follows circular trajectory with a radius of $1.5v_{LN,1,p}$ as shown in Figure 2.3. Thus the control of the frequency and magnitude control of the output voltage of the inverter can be thought as synthesizing a vector revolving with an angular velocity ω and a magnitude of $1.5v_{LN,1,p}$. From Eq. 2.4 we get

$$\text{Magnitude of } \boldsymbol{v}_{LN,1} = \frac{3}{2} v_{LN,1,p} = \frac{\sqrt{3}}{2} \mathrm{M} K_v V_i \tag{2.12}$$

In the space-vector PWM method, the inverter generates eight voltage vectors, $\boldsymbol{V_0}$ through $\boldsymbol{V_7}$. States $\boldsymbol{V_0}$ and $\boldsymbol{V_7}$ are zero states. The other six states are shown in Figure 2.4. The non zero voltage space vectors divide the complex plane into six 60^o partitions called sextants.

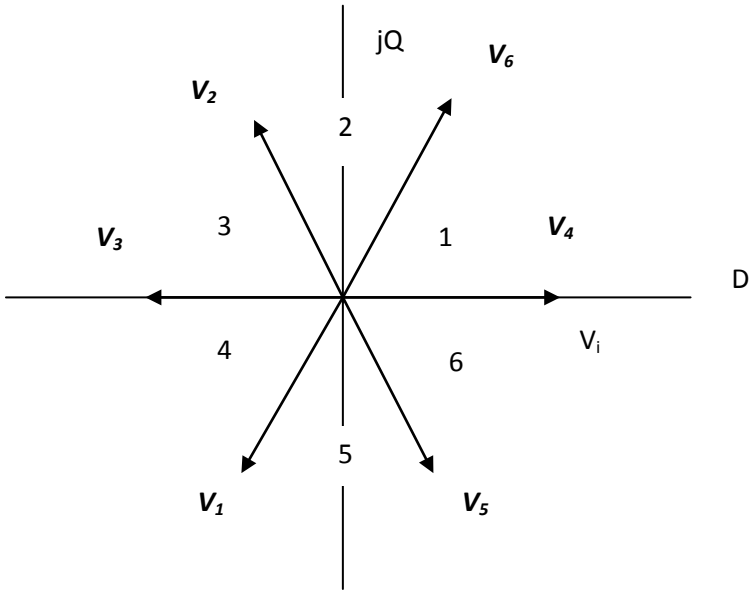

Figure 2.4: Non-zero **v**oltage space vectors of the three phase VSI

Times of individual states are calculated from simple formulas, and in each switching cycle the states follow a specific timed sequence of five or six states [4]. Assuming the voltage space-vector pulse width modulation technique, operation of the circuit in Figure 2.2 was simulated. The power spectral density of the inverter output voltage with the switching frequency of 10 kHz is shown in Figure 2.5. Apart from the fundamental, the rest of the spectrum represents voltage noise.

As seen in Figure 2.5, the power density of the noise peaks up at the multiples of switching frequency. These peaks are resulting from the periodic operation of switches of the inverter. The voltage noise causes current noise and, as a result, electromagnetic noise is emitted from the inverter. The consequent electromagnetic interference (EMI) is a serious practical problem because of its effects on sensitive communication equipment. PWM power electronic converters, used in many industrial, domestic, commercial, and

military applications, are strong sources of EMI. The common hardware solution involves EMI filters, which are inconvenient and costly. A software solution, which is the subject of this thesis, is presented in the subsequent chapters.

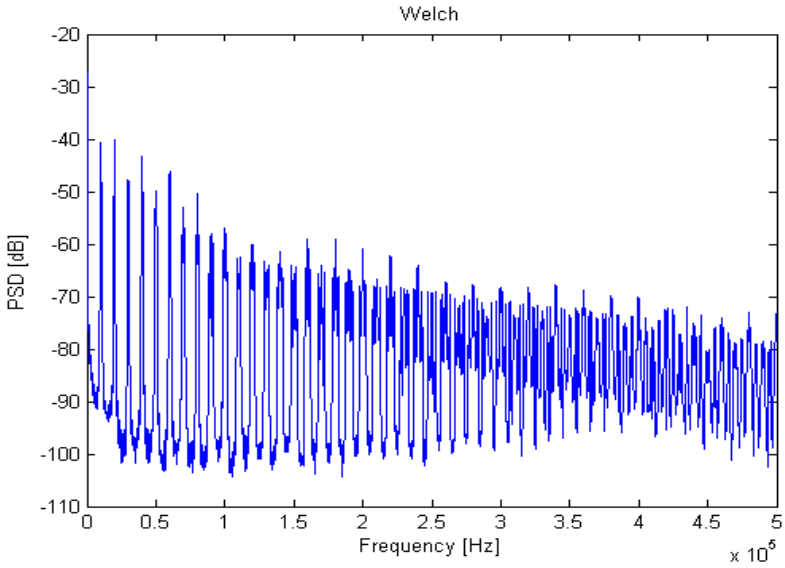

Figure 2.5: Power spectral density (PSD) of the output voltage of an inverter operating with constant switching frequency of 10 kHz.

Chapter 3

Mitigation of EMI

From Chapter 2 we can see that power electronic converters are one of the strongest sources of EMI. Figure 2.6 shows the power spectral density of the output voltage of the inverter; we could see a considerable amount of noise which is the main cause of EMI. The methods for mitigating the EMI are described in this Chapter.

3.1 Filters

The basic solution that comes in to mind in order to mitigate the EMI is filters, because we need to suppress the high frequency harmonic content (higher harmonics of voltages and currents). The filters used to mitigate the EMI noise are also called as EMI filters. The EMI filters are simple inductive and capacitive circuits used to filter out the high frequency components.

The reactance of the capacitor and the inductor depends on the frequency of the input voltage.

For a capacitor, reactance is inversely proportional to the frequency

$$X_c \propto \frac{1}{f} \tag{3.1}$$

$$X_c = \frac{1}{2\pi f C} \tag{3.2}$$

Where X_c is the capacitive reactance of the capacitor,

C is the capacitance of the capacitor and

f is the frequency of the input voltage.

From equation (3.1) it is obvious that a capacitor offers less reactance to high frequency components, i.e., allows only high frequency signals.

For an inductor, reactance is directly proportional to the frequency

$$X_L \propto f \tag{3.3}$$

$$X_L = 2\pi f L \tag{3.4}$$

Where X_L is the inductive reactance of the inductor,

L is the inductance of the inductor and

f is the frequency of the input voltage.

From equation (3.3) we can see that inductor allows only low frequency components.

The capability of the EMI filters is determined by the insertion loss. The EMI filters have insertion loss approximately proportional to LCf^2. The insertion loss is dependent on the frequency, making the EMI filters less effective in mitigating the low-order harmonics of the voltage and current produced by the PWM operated converters. In the present day's PWM converters the switching frequencies are less than 20 kHz, and

cause a major problem in the lower portion of the radio frequency range. Elimination of these harmonics requires high LC valued filters making them bulky and expensive. Thus filters are not a perfect solution for the mitigation of EMI.

3.2 Random Pulse Width Modulation

In the regular space-vector PWM, the active pulse position with respect to the beginning of the period is fixed and the switching frequency is constant. The frequency spectrum of the output of the space-vector PWM inverter contains the harmonic components at switching frequency and its multiples. The random pulse width modulation (RPWM) techniques have been developed in order to reduce or eliminate the harmonic peaks.

To fight the electromagnetic noise produced by the PWM converters an RPWM technique was first proposed in [1] and shown in [5] as an inexpensive and effective means of mitigating the electromagnetic noise. A specific parameter of the PWM technique is varied randomly, due to which non-periodic switching patterns are generated and the discrete harmonic power is transferred to continuous spectrum of the output voltages. Studies published in [2] and [3] have shown that the level of EMI can be reduced by 10-20 dB by using the RPWM techniques. Any PWM strategy with fixed-duration switching cycles can be converted to RPWM, so the space-vector PWM technique is a good choice for RPWM [6], [7].

The voltage source inverter used in used in simulations is shown in figure 2.2. As already explained in Chapter 2 no two switches in the same leg may be ON. Each leg has

two switches, which are controlled by the switching variables *a*, *b* and *c*. The switching variable in the first leg is given by

$$a(t) = \begin{cases} 0 & \text{SA} = \text{OFF},\ \ \text{SA1} = \text{ON} \\ 1 & \text{SA} = \text{ON},\ \ \text{SA1} = \text{OFF} \end{cases} \tag{3.5}$$

The switching variables *b* and *c* are defined similarly, but SA is replaced by SB and SC and SA1 is replaced by SB1 and SC1 respectively.

The duty ratio of a single phase *a (t)* is given by the equation (see [8]):

$$d(t) = \frac{1}{2}[\,1 + MF(t)] \tag{3.6}$$

where *F (t)* is the modulation function,

$-1 < F(t) < 1$ and

M is the modulation index that controls the amplitude of the output voltage.

If $0 < M < 1$, then

$$0 < d(t) < 1 \tag{3.7}$$

For an inverter the modulation is supposed to have a sinusoidal form and is given by

$$F(t,\theta) = \sin(\omega_1 t + \theta) \tag{3.8}$$

where $\omega_1 = 2\pi f_1$,

f_1 is the fundamental output frequency in Hz and

θ is the phase reference.

Therefore, the duty ratio for a single pulse can be expressed as

$$d(t,\theta) = \frac{1}{2}\,[\,1 + M\sin(2\pi f_1 t + \theta)] \tag{3.9}$$

In PWM inverters, the switching frequency (switching rate) is usually fixed and it is much greater than the fundamental output frequency. Their ratio, *N*, defined as

$$N = \frac{f_{sw}}{f_1} \tag{3.10}$$

is also the number of switching intervals contained in an output cycle. The switching interval is the reciprocal of the switching frequency

$$\tau_{sw} = \frac{1}{f_{sw}} \tag{3.11}$$

Equations (3.10) and (3.11) are for a system with fixed switching frequency. For a randomized switching frequency, the randomly changing interval will be denoted by τ_i, whose average value is the statistical expectation of $\tau_{i.}$. The randomized switching frequencies have limitations at both high and low ends. Too high a frequency increases the switching loss and it can be unrealizable in a microcontroller. Too low frequency results in a high current ripple.

According to [9], using discrete random distribution is advantageous over continuous ones, because it is easier to implement and simpler to analyze. If the number of discrete frequencies in the pool is 5 or greater, there seems to have very little difference at the output side compared with the continuous distribution. Some authors even reported use of only 3 frequencies [10]. Furthermore, there can be a weighting

factor for each frequency, and the factors follow a pre-determined desirable distribution [9]. Optimization of switching frequencies in a limited pool is described in [11].

Let us consider time t_m, i.e., the m^{th} interval, which is

$$t_m = \sum_{i=0}^{m=1} \tau_i \tag{3.12}$$

and where the switching interval is τ_m.

The pulse width is then the product of the duty ratio and the switching interval at that time, that is, $d(t_m)\ \tau_m$. A sequence of switching intervals from m^{th} interval to k^{th} interval is illustrated in Figure 3.1. The time between m^{th} interval and k^{th} interval is

$$\gamma_k = \sum_{i=m+1}^{m+k-1} \tau_i \tag{3.13}$$

and the time from m^{th} interval to k^{th} interval is

$$\delta_k = \sum_{i=m+1}^{m+k-1} \tau_i + \frac{\tau_m + \tau_{m+k}}{2} \tag{3.14}$$

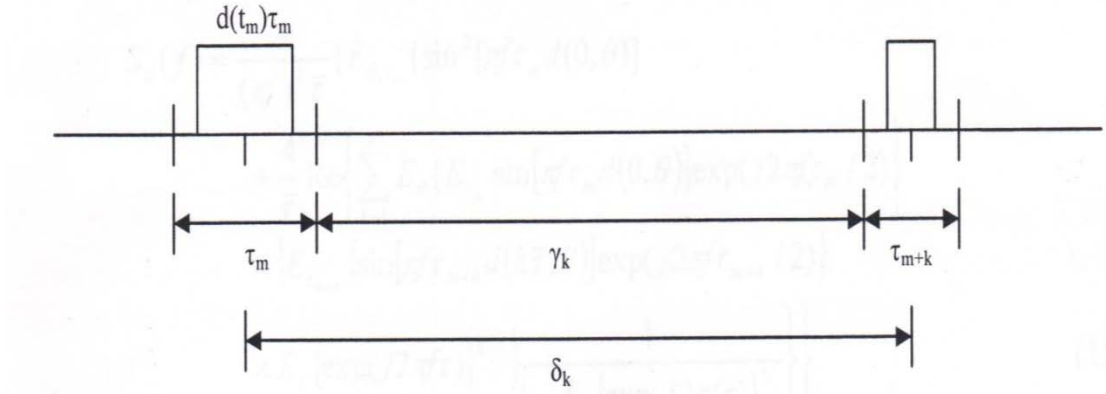

Figure 3.1: A train of random switching intervals with the pulses aligned in the center of each interval (notice that the m^{th} and k^{th} interval are of different length, and that the duty ratios of the two pulses are not necessarily the same).

Because of the stationary and ergodic characteristics of the sequence, the autocorrelation is given by

$$R(\tau) = \lim_{T\to\infty} \frac{1}{T}\int_0^T E[v(t)v(t-\tau)]\,dt \tag{3.15}$$

For the line-line voltages, $v(t) = v_{ab}(t)$, or $v(t) = v_{bc}(t)$, or $v(t) = v_{ca}(t)$, and for the line to neutral voltages, $v(t) = v_a(t)$, or $v(t) = v_b(t)$, or $v(t) = v_c(t)$. The spectral density function is the Fourier transform of autocorrelation

$$S(f) = \int_{-\infty}^{\infty} R(\tau)e^{-j2\pi f\tau}\,d\tau \tag{3.16}$$

A general formula for power spectral density of the per unit line to line voltage ($a(t) - b(t)$) was derived in [9] as

$$S_{ab}(f) = \frac{4}{(\pi f)^2 \bar{\tau}} \{E_{\theta,\tau_m}\{\sin^2[\pi f \tau_m d(0,\theta)]$$

$$-\sin[\pi f \tau_m d(0, \theta - \tfrac{2}{3}\pi)] \sin[\pi f \tau_m d(0, \theta)]$$

$$+ 2\mathrm{Re}\{\sum_{k=1}^{N} E_\theta\{E_{\tau_m}\{\{\sin[\pi f \tau_m d(0, \theta)]$$

$$-\sin[\pi f \tau_m d(0, \theta - \tfrac{2}{3}\pi)]\} \exp(j2\pi f \tau_m/2)\}$$

$$\times \{E_{\tau_{m+k}}\{\sin[\pi f \tau_{m+k} d(k\bar{\tau}, \theta)] \exp(j2\pi f \tau_{m+k}/2)$$

$$\times E_\tau\{\exp(j2\pi f\tau)\}^{k-1}\} \frac{1}{1 - E_\tau\{\exp(j2\pi f\tau)\}^N}\}\} \quad (3.17)$$

Similarly, the general formula for power spectral density of the per unit line to neutral voltage (a (t)) was expressed in [9] as

$$S_a = \frac{4}{(\pi f)^2 \bar{\tau}} \{E_{\theta,\tau_m}\{\sin^2[\pi f \tau_m d(0, \theta)]$$

$$+ \frac{4}{\bar{\tau}} Re\{\sum_{k=1}^{N} E_\theta\{E_{\tau_m} \sin[\pi f \tau_m d(0, \theta)] \exp(j2\pi f \tau_m/2)\}$$

$$\times \{E_{\tau_{m+k}}\{\sin[\pi f \tau_{m+k} d(k\bar{\tau}, \theta)] \exp(j2\pi f \tau_{m+k}/2)\}$$

$$\times E_\tau\{\exp(j2\pi f\tau)\}^{k-1}\} \frac{1}{1 - E_\tau\{\exp(j2\pi f\tau)\}^N}\}\} \quad (3.18)$$

It can be seen that pulse width modulation can only affect the low-frequency EMI. The high frequency noise still requires EMI filters. However, the required values of *LC* for those filters are low, resulting in reduction of size and cost of the filters.

Chapter 4

Random Pulse Width Modulation

The RPWM techniques were developed in order to reduce or eliminate the higher harmonics. These techniques have an advantageous effect on acoustic and electromagnetic noise produced by the inverter. There are two types of RPWM techniques. They will be discussed in the following section.

4.1 RPWM Techniques

There are two types of RPWM techniques:

1. Random pulse position modulation: In this type of modulation the switching frequency (f_{sw}) is maintained constant and the active pulse position with respect to the beginning of the switching period is randomly selected. The power spectral density (PSD) for random pulse position modulation is given by [12],[13]:

$$P_{vab}(f) = V_{dc}^2 \frac{\sin^2(\pi f t_{on})}{T_{sw}\pi^2 f^2}\left(1 - \left|E(e^{-j2\pi f\Delta})\right|^2 + \frac{1}{T_{sw}}\left|E(e^{-j2\pi f\Delta})\right|^2 \sum_{n=-\infty}^{\infty} \delta\left(f - \frac{n}{T_{sw}}\right)\right) \quad (4.1)$$

where T_{sw} is the switching period,

$f_{sw} = 1/T_{sw}$,

E(x) represents the statistical average (expectation),

Δ is the random pulse position respect to the beginning of period, and

δ is the Dirac impulse,

$$\delta(x) = \begin{cases} \infty & x = 0 \\ 0 & x \neq 0 \end{cases} \tag{4.2}$$

The last term in equation 4.2 is a sum of Dirac impulses, from Eq. 4.1 it is clear that the PSD of the random pulse position modulation contains both discrete and continuous harmonic components. Therefore in practical systems this technique is ineffective for harmonic mitigation.

2. Random switching frequency modulation: Whereas in this type of modulation the switching frequencies (f_{sw}) are randomly selected and the active pulse position with respect to the beginning of the switching period is fixed. The PSD in this case is given by [12],[13]:

$$P_{vab}(f) = \frac{V_{dc}^2}{T_{sw}\pi^2 f^2}\left(E(\sin^2(\pi f D\tau)) + 2\Re e\left(\frac{E^2(\sin(\pi f D\tau)e^{j\pi f\tau})}{1 - E(e^{j2\pi f\tau})} \right) \right) \tag{4.3}$$

where T_{sw} is the average switching period,

$T_{sw} = \mathrm{E}(\tau) = \mathrm{E}(1/f_{sw})$,

where E(..) denotes the statistical expectation, and

$\tau = 1/f_{sw}$ is the random switching period.

From equation 4.3 we can see that the PSD of this technique has only the continuous component. Therefore random switching frequency modulation technique is used for the mitigation of harmonic noise and electromagnetic noise.

4.2 Random Switching Frequency Modulation

In order to explain about the random switching frequency modulation technique, we must note that the PWM converter operates with continuous current, whereas the voltage is a train of width modulated pulses. The voltage pulses appear in a sequence of

time intervals called switching intervals. Each switching interval contains a single voltage pulse, and the length of the switching interval is referred to as switching period. The reciprocal of switching period is called switching frequency or switching rate. In this RPWM technique the switching period is randomized in order to transfer the discrete harmonic power to continuous power spectral density.

Thus random switching frequency modulation technique is very effective in mitigating the harmonic and electromagnetic noise produced in PWM inverters. Therefore the random switching frequency modulation technique is well suited for the mitigation of EMI. In simulations, we used this technique to mitigate the electromagnetic noise.

4.3 Spectral Nulls

The basic objective of the described project was to minimize the spectral power density at a desired frequency f_0 and its multiples kf_0, and these dips in the spectrum are called spectral nulls. The nulls can be used as communication channels by the integrated communication systems, and keep power away from the harmful frequencies for the environment (EMI, acoustic noise) or the system (resonant frequencies).

In order to get the spectral nulls the power density P_{vab} in Eq. 4.3 must be zero. This will occur when both $E(\sin^2(\pi fD\tau))$ and $E^2(\sin^2(\pi fD\tau)e^{j\pi f\tau})$ are zero for a given D and f. So the random variable τ must be selected in such a way that the following condition is always true for the frequency $f = f_0$:

$$\sin(\pi fD\tau) = 0 \tag{4.4}$$

From equation 4.4 we can get the following condition

$$\pi f D \tau = k\pi \tag{4.5}$$

$$\tau_{x,y,z} = \frac{1}{f_{sw}} = \frac{k}{f_0 D_{a,b,c}} \ , k = 1,2,3... \tag{4.6}$$

where D_a, D_b, D_c, are the duty cycles of the respective inverter voltages.

The line voltage duty cycles that satisfy Eq. 4.6 are

$$D_{ab} = \frac{1}{2} | D_a - D_b | \tag{4.7}$$

$$D_{bc} = \frac{1}{2} | D_b - D_c | \tag{4.8}$$

$$D_{ca} = \frac{1}{2} | D_c - D_a | \tag{4.9}$$

The frequency cancellation at a desired frequency may be acquired either by single phase or three phase perspectives.

I. In the single phase approach, the frequency cancellation occurs only on one phase and an algorithm for this is as follows

   a) For each particular phase the minimum switching period is selected according to Eq. 4.6 by considering the appropriate duty cycle.

   b) The actual switching period is computed by randomly selecting a multiplier *k* from a pool of integer values.

c) Thus for all three phases the calculated switching period is taken as the PWM switching period.

d) By taking the phase duty cycles D_a, D_b, D_c into consideration the PWM signal is generated.

II. In the three phase approach, the frequency cancellation occurs in all three phases simultaneously and an algorithm for this is as follows

a) Whereas in this case the minimum switching period for each phase is selected according to Eq. 4.6, by considering all the three duty cycles from Eqs. 4.7, 4.8 and 4.9.

b) The minimum switching periods obtained are rounded to integer numbers and are multiplied by a scale factor of convenient magnitude.

c) The least common multiple of rounded switching periods is selected.

d) The selected least common multiple of the switching periods is used as the PWM switching period for all three phases.

e) By taking the phase duty cycles D_a, D_b, D_c into consideration the PWM signal is generated.

The main drawback for the three phase approach is that the resulting switching period which is obtained as the least common multiple may be very large, so it can be impractical.

An alternative approach for the three-phase cancellation approach might use different switching periods for each phase, as determined from Eq. 4.9. There is no need to determine the least common period multiple. However, setting different switching periods for each phase is rather difficult to implement in a regular digital signal processing (DSP) controller with PWM support.

The described technique would only affect the low frequency EMI, but the high frequency content can easily be eliminated using small EMI filters. In this way, cost and size of the filter can be effectively reduced. The simulation program and results are discussed in the subsequent Chapter.

Chapter 5

Simulation Program: Implementation and Results

This Chapter discusses the way in which the simulation program was implemented. The simulation program was based on the analysis done on RPWM in Chapter 4. The simulation results are discussed after the program description.

5.1 Simulation Program

The flow charts of the simulation program implemented in MATLAB are shown in Figures 5.1 and 5.2. Figure 5.1 shows the flow chart of the simulation program implemented in MATLAB for space-vector PWM (for a constant switching frequency). Whereas the Figure 5.2 shows the flow chart of the simulation program implemented in MATLAB for RPWM (random switching frequency modulation). The frequency cancellation (spectral nulls) for a three-phase inverter has been simulated by following the single-phase approach for the line voltages.

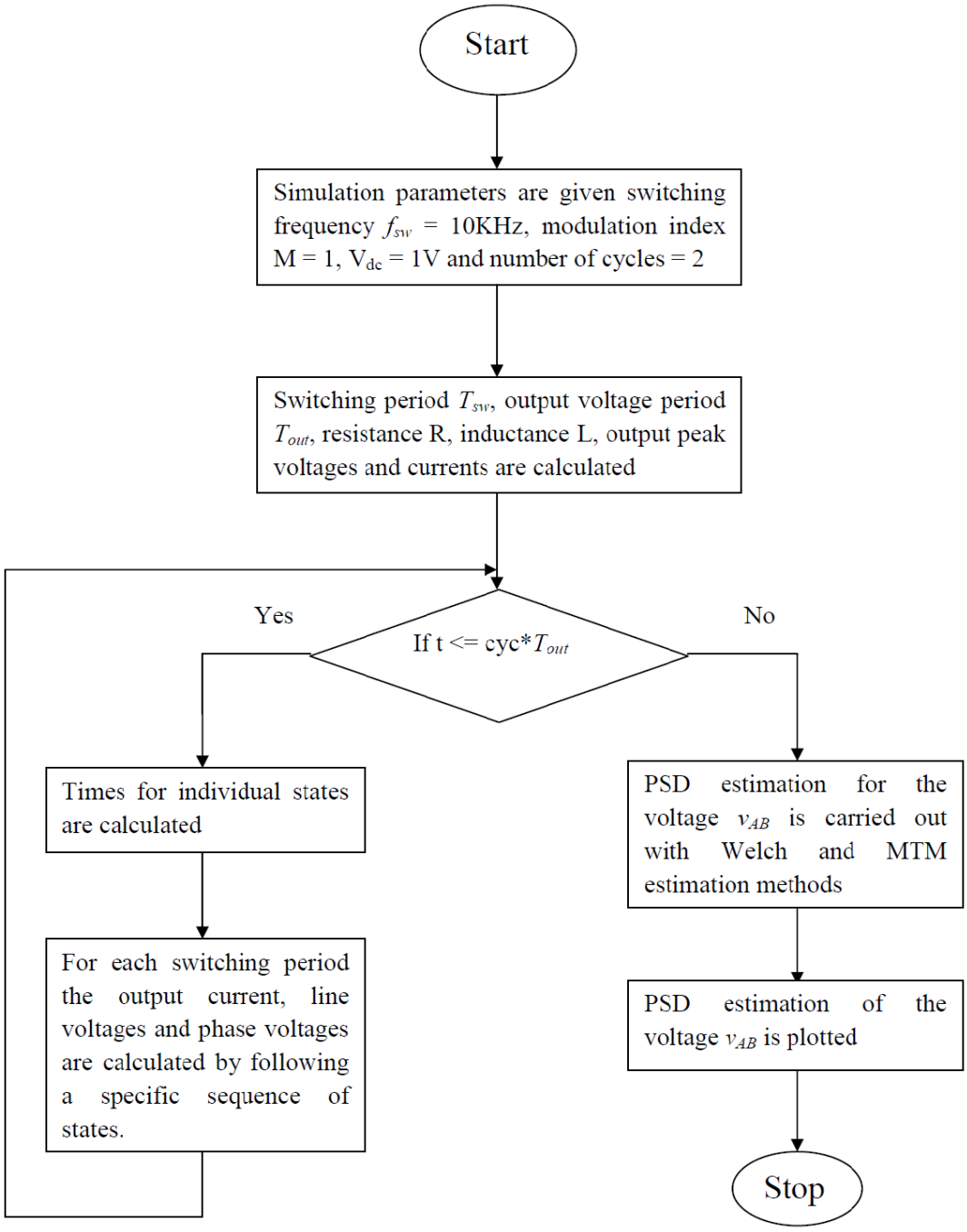

Figure 5.1: Flow chart for MATLAB simulation of space vector PWM technique

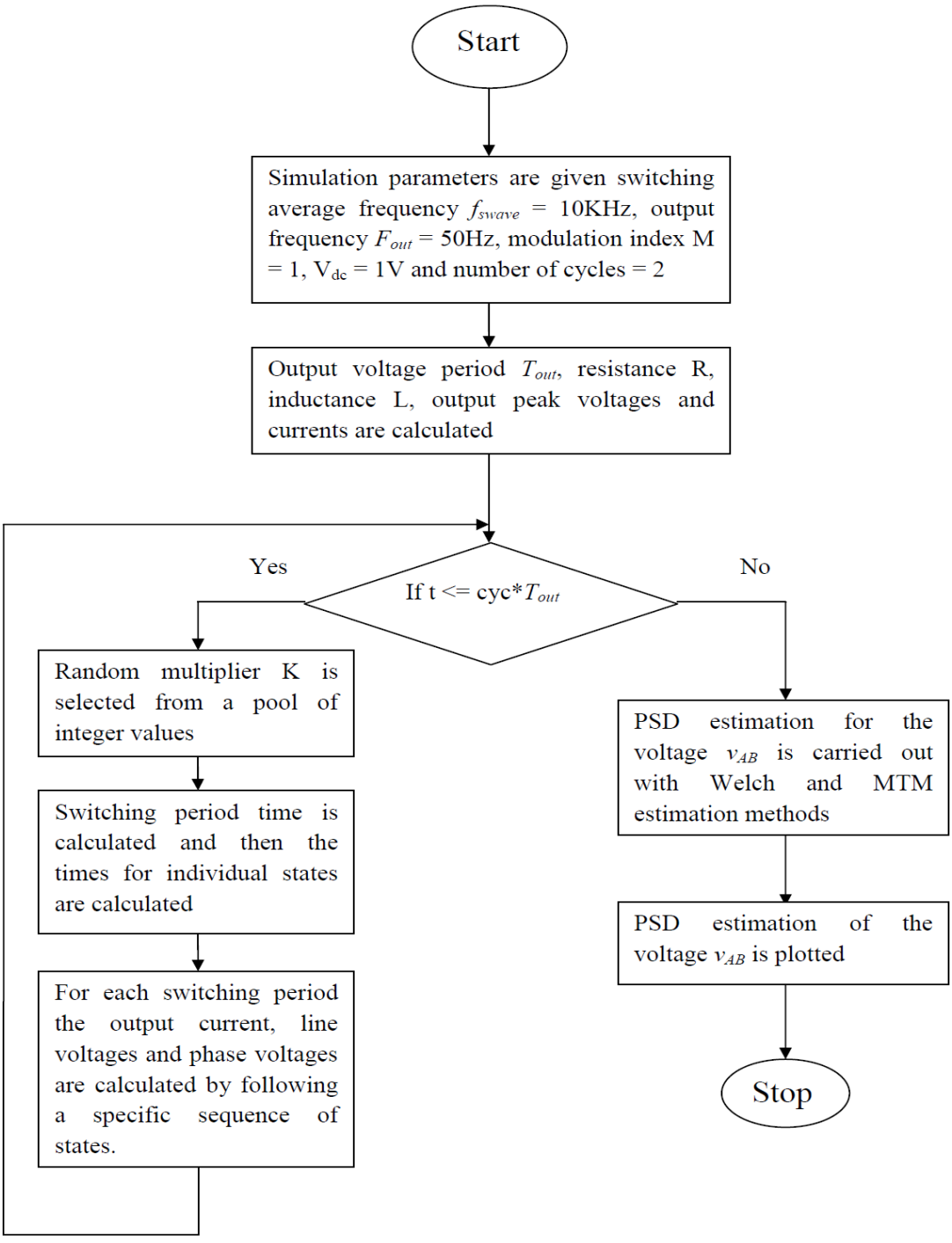

Figure 5.2: Flow chart for MATLAB simulation of RPWM technique

5.2 Simulation Results

Simulation of an inverter operating with constant switching frequency and space vector PWM, gave the following results with the MTM and Welch estimation methods:

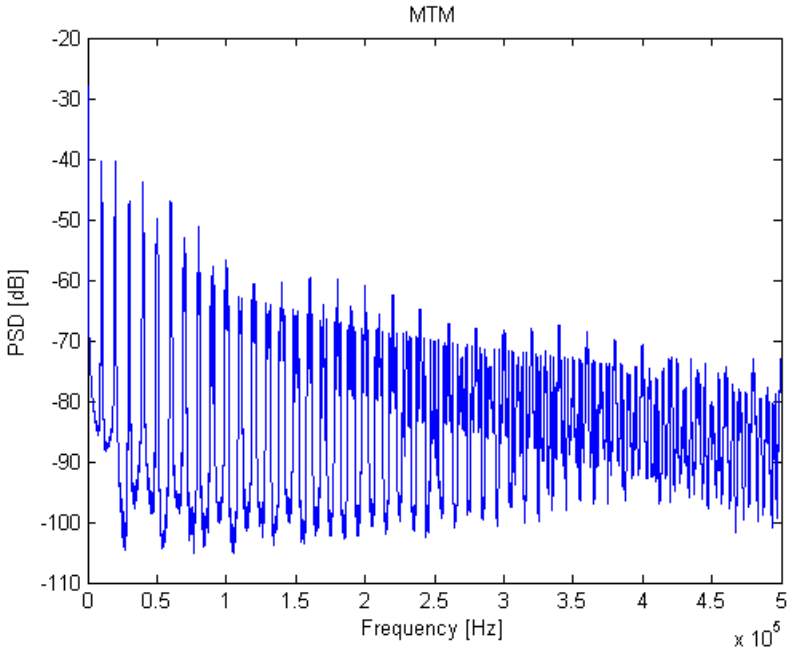

Figure 5.3: PSD with MTM estimation of deterministic PWM.

Figure 5.3 shows the PSD with MTM estimation of the deterministic PWM for switching frequency, f_{sw} = 10 kHz. Figure 5.4 shows the PSD with Welch estimation of the deterministic PWM for switching frequency, f_{sw} = 10 kHz.

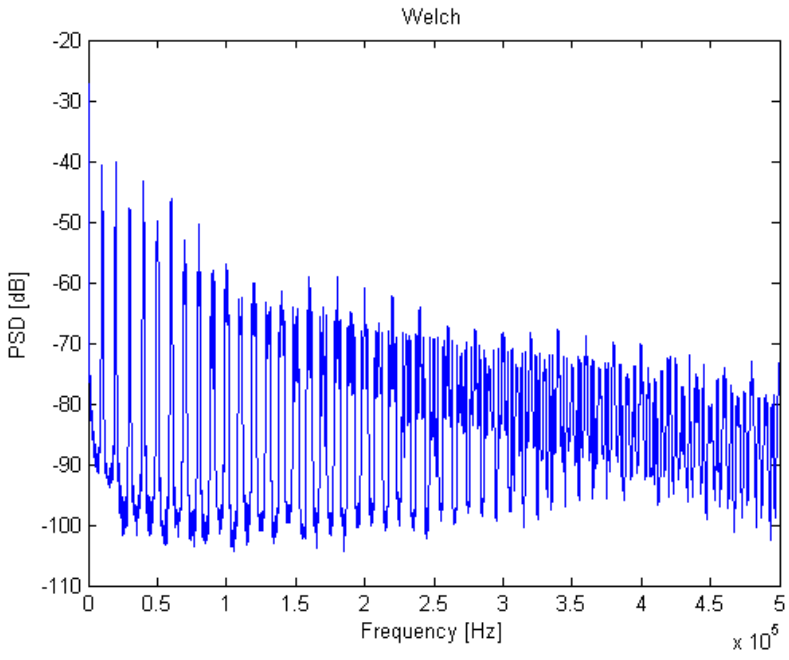

Figure 5.4: PSD with MTM estimation of deterministic PWM.

Simulation of an inverter operating with RPWM without spectral nulls: In this section we used the standard RPWM technique. These simulations were done for comparison. The switching period pools using the random multiplier *k* sets given by Eq. 5.1 and 5.3 were used respectively. Figures 5.5 and 5.6 show the PSD with MTM estimation of RPWM without spectral nulls using Eqs. 5.1 and 5.3, respectively

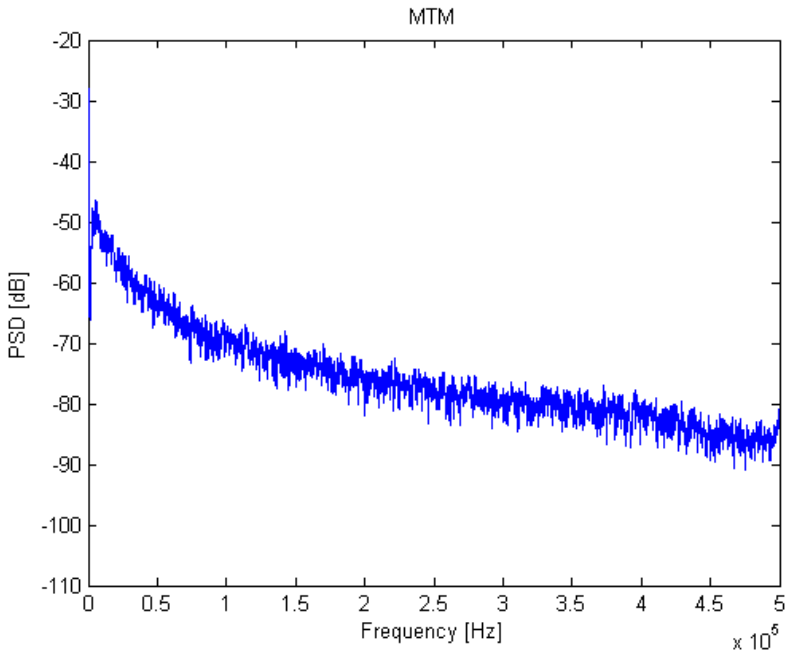

Figure 5.5: PSD with MTM estimation of RPWM without spectral nulls using Eq. 5.1.

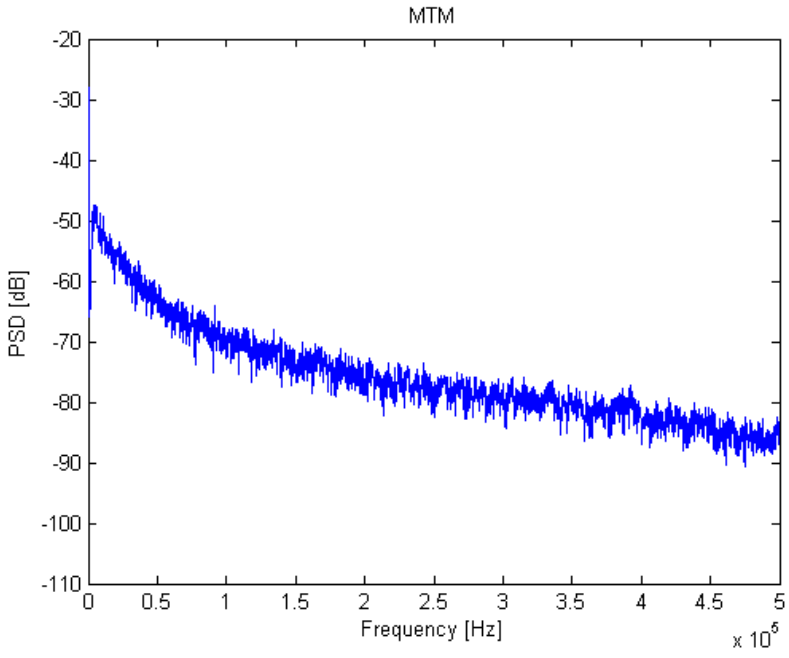

Figure 5.6: PSD with MTM estimation of RPWM without spectral nulls using Eq. 5.3.

Figures 5.7 and 5.8 show the PSD with Welch estimation of RPWM without spectral nulls using Eqs. 5.1 and 5.3, respectively.

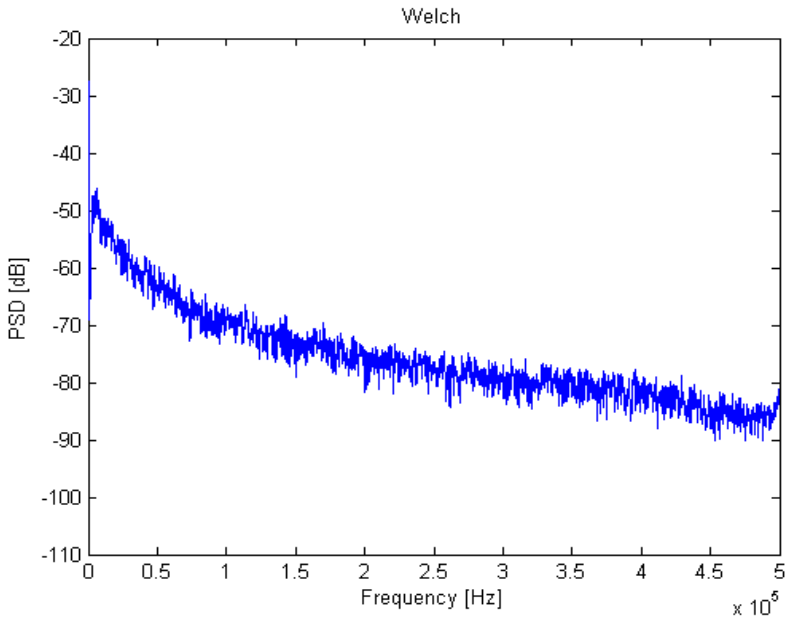

Figure 5.7: PSD with Welch estimation of RPWM without spectral nulls using Eq. 5.1.

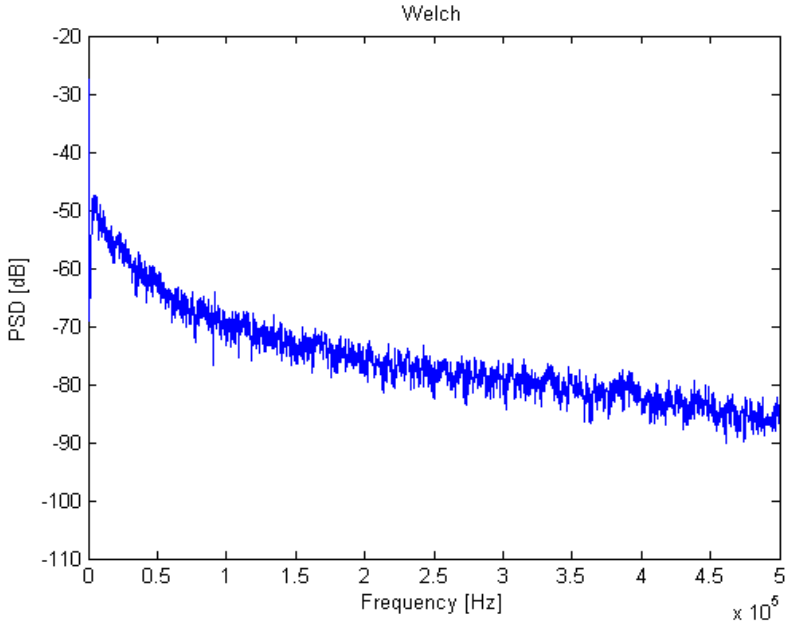

Figure 5.8: PSD with Welch estimation of RPWM without spectral nulls using Eq. 5.3.

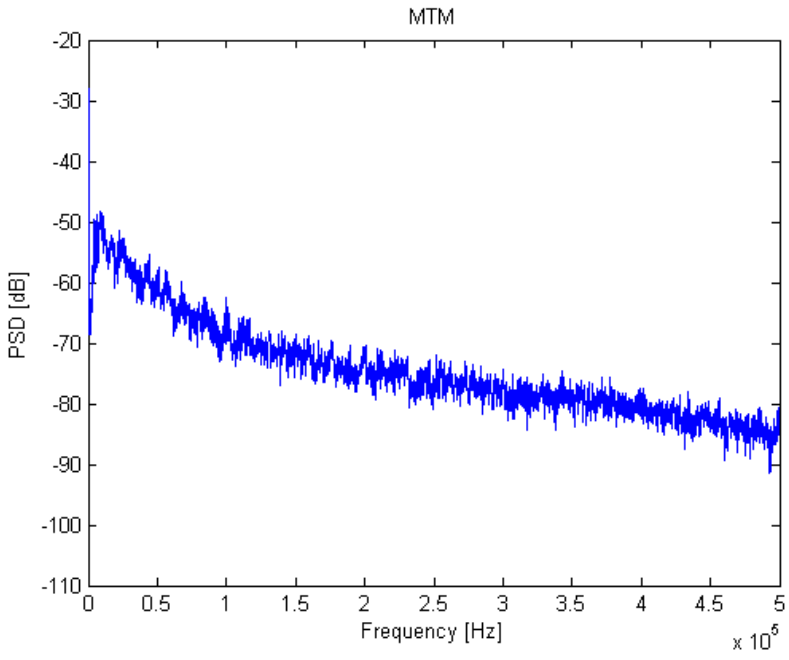

Figure 5.9: PSD with MTM estimation of RPWM without spectral nulls, with experimental switching periods.

With the switching-period pool used in experiments

T_{sw} = 70, 80, 90, 100, 120, 140, 180, 240 [μs], (5.9)

the results are shown in Figures 5.9 and 5.10. Figure 5.9 shows the PSD with MTM estimation of RPWM without spectral nulls, by using the switching periods used in experiments. Figure 5.10 shows the same result but using the Welch method.

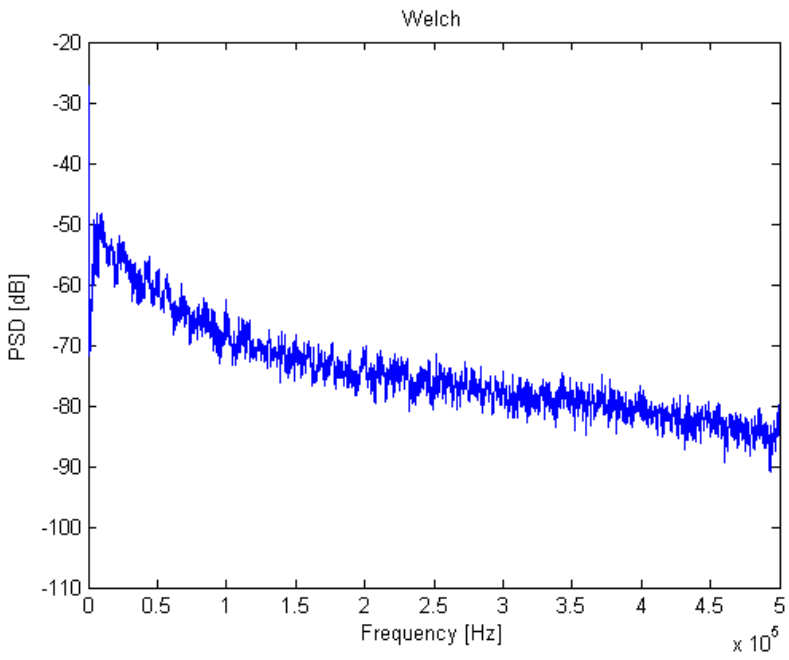

Figure 5.10: PSD with Welch estimation of RPWM without spectral nulls, with experimental switching periods.

The PSD with MTM and Welch estimation of the RPWM with spectral nulls, where the cancellation frequency f_0 = 150 kHz, is given in Figures 5.11, 5.12, 5.13 and 5.14. Figures 5.11 and 5.12 correspond to the first set random multiplier *k* integer values given by Eq. 5.1, where Figure 5.11 shows MTM estimation of PSD and Figure 5.12 shows the Welch estimation of PSD. Figures 5.13 and 5.14 correspond to the second set of random multiplier *k* integer values given by Eq. 5.3, where Figure 5.13 shows MTM estimation of PSD and Figure 5.14 shows the Welch estimation of PSD.

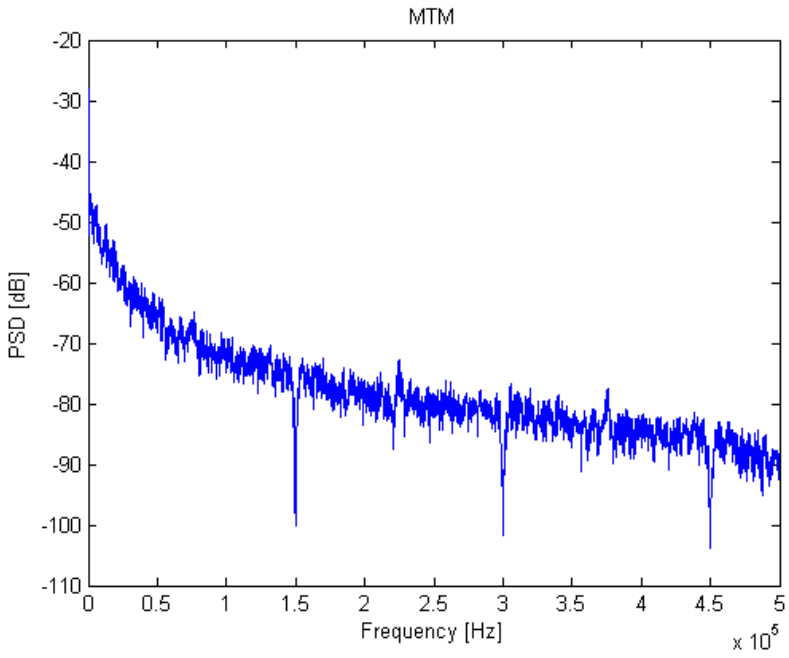

Figure 5.11: PSD with MTM estimation of RPWM with spectral nulls using Eq. 5.1.

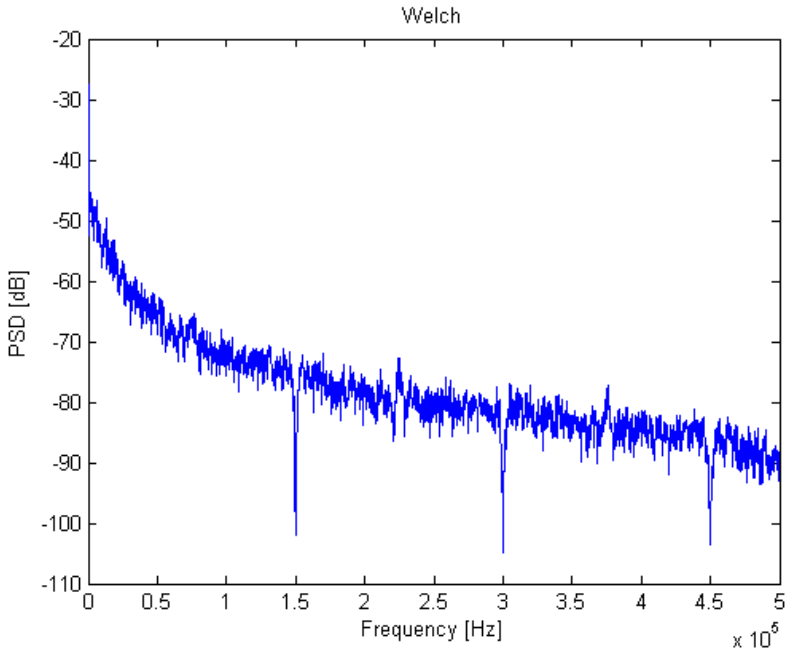

Figure 5.12: PSD with Welch estimation of RPWM with spectral nulls using Eq. 5.1.

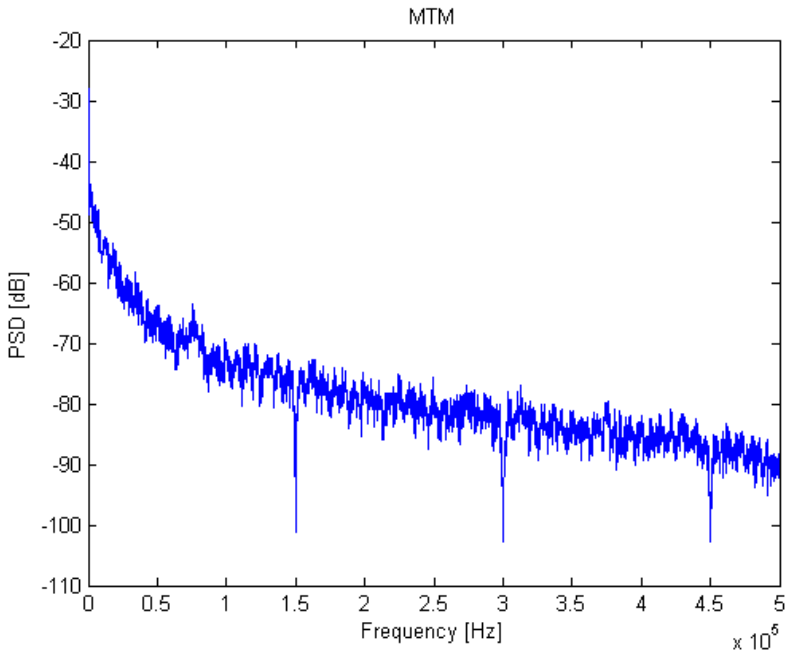

Figure 5.13: PSD with MTM estimation of RPWM with spectral nulls using Eq. 5.3.

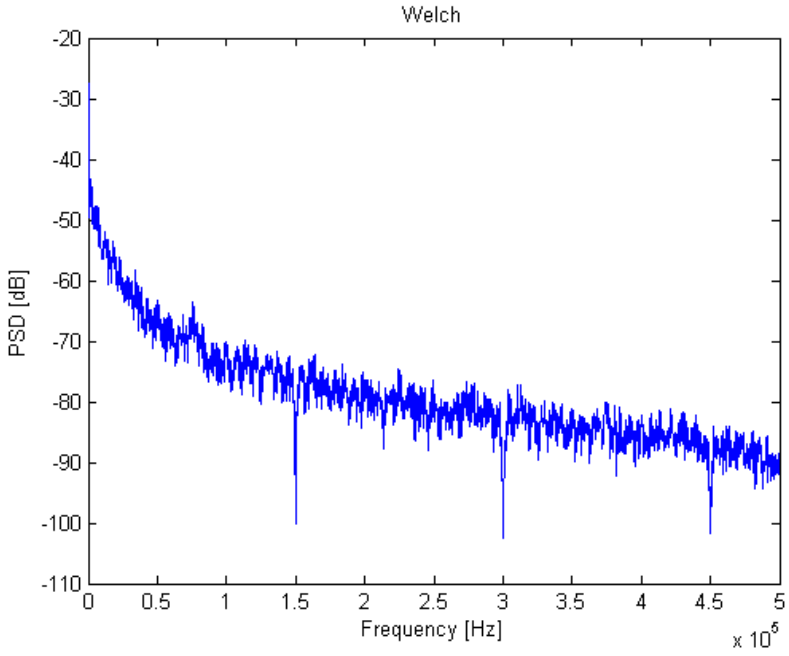

Figure 5.14: PSD with Welch estimation of RPWM with spectral nulls using Eq. 5.3.

Figures 5.3 and 5.4 show the PSD with MTM and Welch estimation of the deterministic PWM, and strong EMI can clearly be seen. Figures 5.5 to 5.10 show the PSD with MTM and Welch estimation of RPWM without spectral null. These figures show that the effects of EMI have been remarkably mitigated. Figures 5.11 to 5.14 show the PSD with MTM and Welch estimation of RPWM with spectral nulls at every 150 kHz.

Chapter 6

Experimental Setup and Results

This chapter describes the experimental setup, implementation details, and the experimental results, which are shown and discussed in the final section.

6.1 Experimental Setup

The block diagram of the experimental setup is shown in Figure 6.1

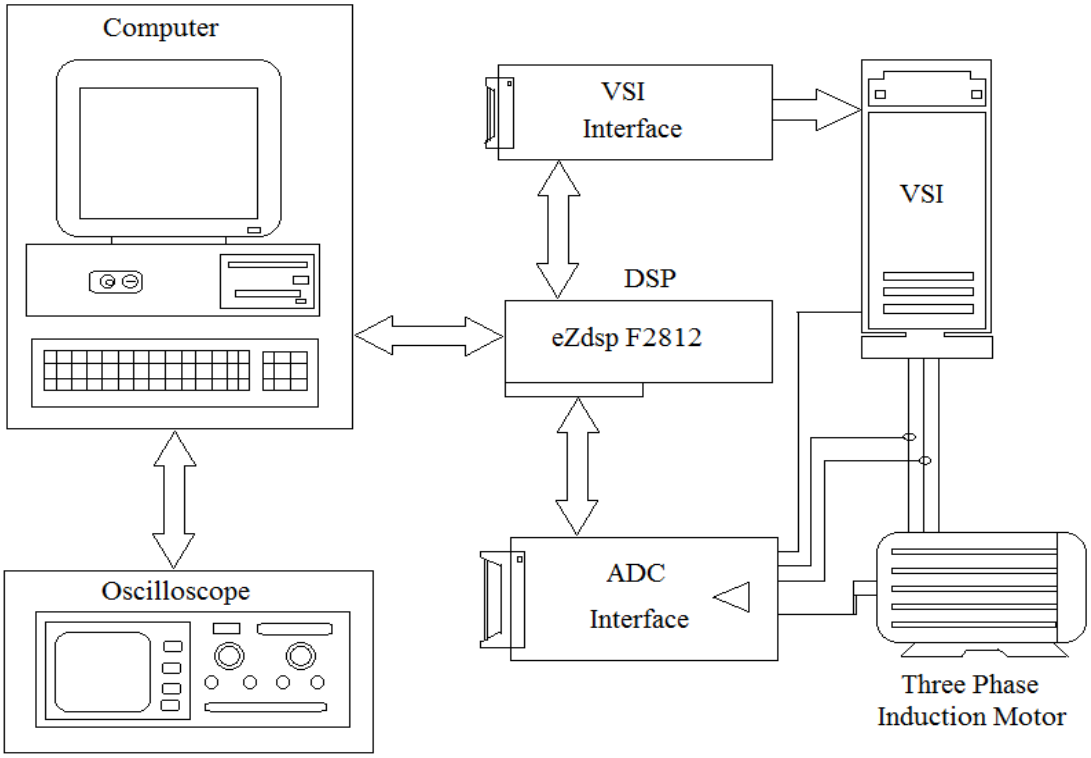

Figure 6.1: Block diagram of the experimental setup.

The experimental setup was composed of:

1. Three phase induction motor with nameplate data:

   P_N = 0.75 hp, V_N = 230/460 V, I_N = 2.3/1.15 A;
2. Industrial VSI with nameplate data:

   Type: Danfoss VLT5004, P_N = 3 hp, V_N = 380-440 V, I_N = 5.6-4.8 A;
3. Digital signal processor control board eZdsp F2812. It contains the TMS320F21812 DSP from Texas Instruments. The eZdsp board is a standalone evaluation module for the F2812 DSP, manufactured by Spectrum Digital.
4. Analog to digital conversion (ADC) interface;
5. Voltage source inverter (VSI) interface;
6. Computer and instrumentation.

The ADC interface and the VSI interface were located on a custom designed extension board. The extension board provided the interface between the eZdsp F2812 module and the system under test. It had three main functions:

1. PWM link which sent the signals from DSP to VSI. The link was realized using a fiber optic interface.
2. Signal processing and acquisition of measured signals. The signals of interest were the inverter output voltages and currents.
3. Serial Communication between the PC and the eZdsp board.

6.2 Experimental Results

The voltage noise spectrum for a constant switching frequency PWM is shown in Figures 6.2 and 6.3. The switching frequency is f_{sw} = 10 kHz, and the fundamental frequency f_1 = 25 Hz for Figure 6.2 and f_1 = 50 Hz for Figure 6.3

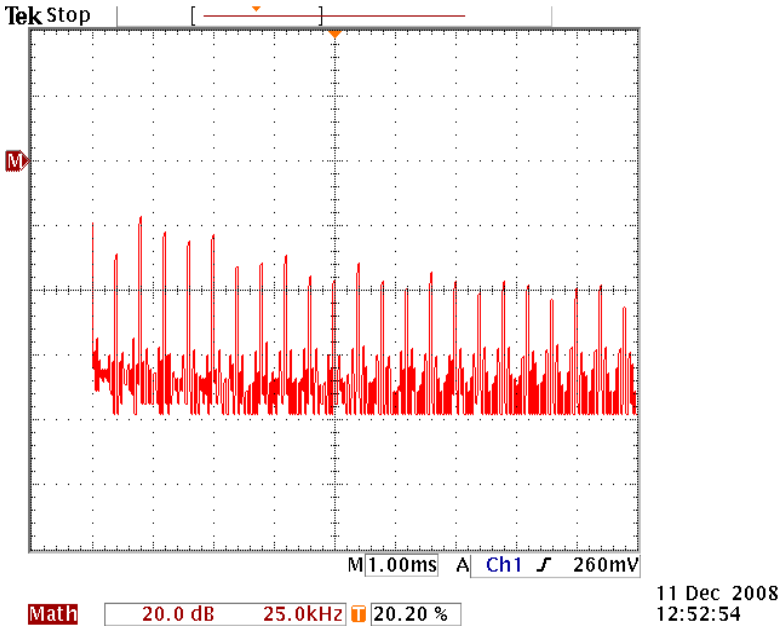

Figure 6.2: Voltage noise spectra for a constant switching frequency PWM, with fundamental frequency f_1 = 25 Hz.

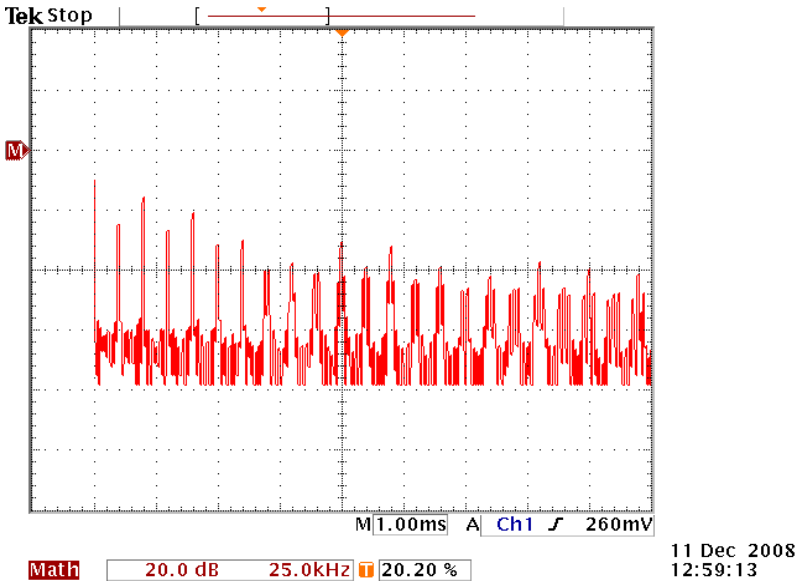

Figure 6.3: Voltage noise spectra for a constant switching frequency PWM, with fundamental frequency f_1 = 50 Hz.

Voltage noise spectrum for RPWM without spectral nulls with fundamental frequency f_1 = 25 Hz is shown in Figure 6.4 and with f_1 = 50 Hz in Figure 6.5.

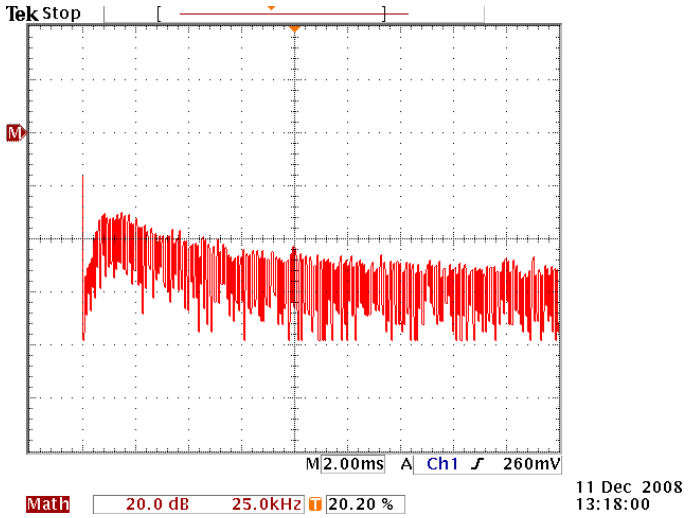

Figure 6.4: Voltage noise spectra for RPWM without spectral nulls, with fundamental frequency f_1 = 25 Hz.

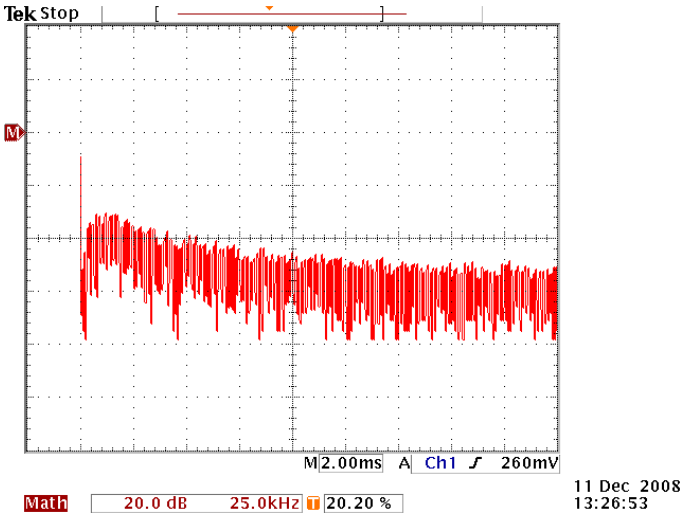

Figure 6.5: Voltage noise spectra for RPWM without spectral nulls, with fundamental frequency f_1 = 50 Hz.

Voltage noise spectrum for RPWM with the spectral null at f_0 = 100 kHz and fundamental frequency f_1 = 25 Hz is shown in Figure 6.6 and with f_1 = 50 Hz in Figure 6.7.

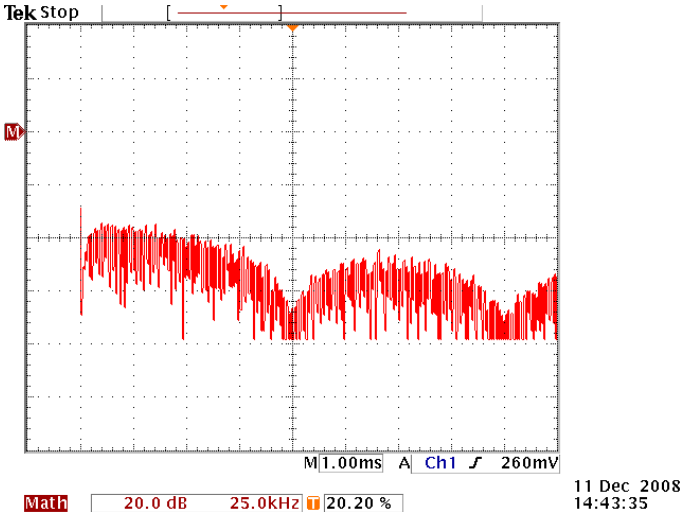

Figure 6.6: Voltage noise spectra for RPWM with spectral nulls at f_0 = 100 kHz, with fundamental frequency f_1 = 25 Hz.

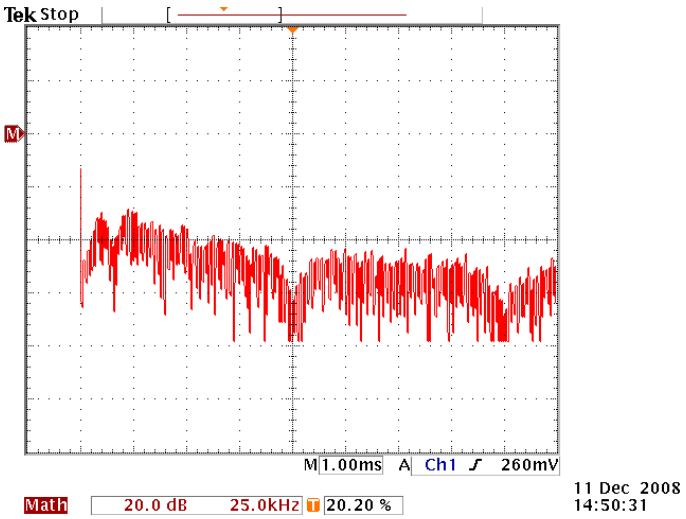

Figure 6.7: Voltage noise spectra for RPWM with spectral nulls at f_0 = 100 kHz, with fundamental frequency f_1 = 50 Hz.

The Figures 6.2 and 6.3 illustrate the classic, non-random PWM. When they are compared with Figures 6.4 - 6.7, the EMI mitigation is easily observed. The spectral nulls are generated every 100 kHz.

Chapter 7

Conclusion

Chapter 1 and 2 describe the PWM inverter and the EMI produced by PWM inverter, because of the fast state transition during the turn-on and turn-off. Chapter 3 shows that RPWM is an effective method to mitigate EMI. Using RPWM, the EMI can be suppressed without increasing the cost and size of the inverter. In contrast with the standard PWM techniques with fixed switching periods, in RPWM, lengths of the switching periods are randomized. If spectral nulls are generated at a desired frequency f_0 and its multiples, they could be used for communication channels. Thus communication systems and power lines can be integrated without polluting the power system with harmful frequencies.

Figures 5.3 and 5.4 in Chapter 5 show simulation results of an inverter controlled by the standard PWM technique. They show significant EMI in the output voltage. These figures can be compared with Figures 5.5 to 5.8 showing simulation results of an inverter using the RPWM with two different sets of values of the random variable *k*. It can clearly be seen that the amount of EMI became considerably reduced. Figures 5.11 to 5.14 show the noise spectra for an inverter using the RPWM technique with two different sets of values of *k*, but with spectral nulls at a desired frequency and its multiples obtained by relating the duty cycle to the length of the switching period. Thus, the modified RPWM

technique has been shown to be effective in reducing the EMI, and the spectral nulls generated can be used for communication channels without affecting the power transfer.

An experimental setup was designed and implemented as described in Chapter 6. Figures 6.2 and 6.3 show the experimental results for an inverter using the standard PWM technique, but with two different fundamental frequencies. Analogous results for an inverter using the RPWM technique are shown in Figures 6.4 and 6.5. It can be seen that the RPWM technique is very effective in mitigating the EMI. Figures 6.6 and 6.7 show the results for an inverter controlled by the modified RPWM technique with spectral nulls at a desired frequency and its multiples.

Among the existing multitude of PWM methods, the new RPWM technique is unique in its interdependency between the duty cycle and switching period. From the results shown in chapters 5 and 6 we can see that lower order of the EMI is mitigated effectively. The lower order harmonics very harmful for communication systems and hence this method is very effective for the mitigation of lower order harmonics. The spectral nulls produces in the RPWM technique can be used as communication channels without affecting the power lines.

The limitations of this technique are that only the low-frequency EMI is affected, that is, that resulting from the current and voltage harmonics associated with the PWM operation of power electronic converters. In order minimize the high frequency content of the noise EMI filters are still necessary. However, because of the high frequency the total LC value of the filters required is low, as is the cost and size of the filters.

From the simulation and experimental results it can be seen that the spectral nulls obtained are very narrow. Further work is thus needed to widen the spectral nulls, that is, replacing them with null bands. Also, expansion of the technique on all three line-to-line voltages is difficult. Either the switching periods must be excessively long, or digital implementation of the modulation strategy would require an excessive amount of real-time computations. Further technological progress in the areas of digital processors and fast semiconductor power switches digital processors may help make these techniques feasible in the near future.

References

1. A. M. Trzynadlowski, S. Legowski, and R. L. Kirlin, "Random pulse width modulation technique for voltage-controlled power inverters," *Conf. Rec. 1987 IEEE Ind. Appl. Soc. Ann. Mtg.*, Atlanta, Georgia, Oct. 1987, pp. 863-868.
2. K. Borisov, T. Calvert, J. A. Kleppe, E. Martin, and A. M. Trzynadlowski, "Experimental investigation of a naval propulsion drive model with the PWM-based attenuation of the acoustic and electromagnetic noise," to appear in *IEEE Trans. Ind. Electron*.
3. A. M. Trzynadlowski, Z. Wang, J. M. Nagashima, C. Stancu, and M. H. Zelechowski, "Comparative investigation of PWM techniques for a new drive for electric vehicles," *IEEE Trans. Ind. Appl.*, 39, 5, pp. 1396-1403, Sep./Oct. 2003.
4. Andrzej M. Trzynadlowski, "Introduction to Modern Power Electronics", New York, Wiley, c1998.
5. A. M. Trzynadlowski, M. Zigliotto, and M. M. Bech, "Random pulse width modulation quiets motors, reduces EMI," *PCIM Power Electron. Syst. Mag.*, pp. 55-58, Feb. 1999.
6. R. L. Kirlin, M. M. Bech, and A. M. Trzynadlowski, "Analysis of power and power spectral density in PWM inverters with randomized switching frequency," *IEEE Trans. Ind. Electron*., 49, 3, pp. 486-499, Apr. 2002.

7. A. M. Trzynadlowski, K. Borisov, Y. Li, and L. Qin, “A novel random PWM technique with low computational overhead and constant sampling frequency for high-volume, low-cost applications,” *IEEE Trans. Power Electron.*, vol. 20, no. 1, pp. 116-122, Jan. 2005.
8. R. L. Kirlin, M. M. Bech, and A. M. Trzynadlowski, “Analysis of power and power spectral density in PWM inverters with randomized switching frequency,” *IEEE Trans. Ind. Electron.*, vol. 49, no. 2, pp. 486-499, 2002.
9. Michael M. Bech, “Random Pulse-Width Modulation Techniques for Power Electronic Converters”, Ph.D. dissertation, Aalborg University, Aalborg East, Denmark, 2000.
10. Andrzej M. Trzynadlowski, “Contol of Induction Motors”, Academic Press, 2001.
11. A. M. Trzynadlowski, M. M. Bech, F. Blaabjerg, J. K. Pedersen, R. L. Kirlin, and M. Zigliotto, “Optimization of switching frequencies in the limited-pool random space vector PWM strategy for inverter-fed drives,” *IEEE Trans. Power Electron.*, vol. 16, no. 6, pp. 852-857, 2001.
12. C. Lascu, A. M. Trzynadlowski, R. L. Kirlin, “Shaping of the noise spectrum in power electronic converters,” Applied Power Electronics Conference and Exposition (APEC), 2010 Twenty-Fifth Annual IEEE, pp. 1749-1754, 2010.
13. R. Lynn Kirlin, Cristian Lascu, Andrzej M. Trzynadlowski, “Shaping the noise spectrum in power electronic converters,” *IEEE Trans.* Industrial Electronics, vol. 99, 2010.